Journal of Computational Physics 425 (2021) 109889

Contents lists available at ScienceDirect

Journal of Computational Physics

www.elsevier.com/locate/jcp

Energetic stable discretization for non-isothermal electrokinetics model ☆

Simo Wu [a], Chun Liu [b], Ludmil Zikatanov [a,*]

[a] Department of Mathematics, Pennsylvania State University, University Park, PA 16802, USA
[b] Department of Applied Mathematics, Illinois Institute of Technology, Chicago, IL 60616, USA

ARTICLE INFO

Article history:
Received 20 November 2019
Received in revised form 21 June 2020
Accepted 28 September 2020
Available online 2 October 2020

Keywords:
PNP (Poisson-Nernst-Planck)
Non-isothermal
Finite element
Energy stable
Math-biology

ABSTRACT

We propose an edge averaged finite element (EAFE) discretization to solve the Heat-PNP (Poisson-Nernst-Planck) equations approximately. Our method enforces positivity of the computed charged density functions and temperature function. Also the thermodynamic consistent discrete energy estimate which resembles the thermodynamic second law of the Heat-PNP system is prescribed. Numerical examples are provided.

1. Background

The study of thermodynamic properties of complex fluid involving electrical solvent is of interest of many biological and physiological applications [1–3]. For example, electrokinetic microfluidic devices have been widely used in biomedical and biotechnological applications and chemical synthesis, which can be used for pumping and controlling the liquid flow in microfluidic systems or separating constituents suspended in a liquid [2,4]. While low thermal conductivity devices are widely used, temperature effect should be included as it affects the electrical conductivity and can produce substantial heat driven flow. In addition, the interaction between heat flux and electric field could result in Joule heating effect as a byproduct of presence of electric field [5,6]. This effect is generated by the ohmic resistance of the electrolyte subjected to electric current and, clearly, the traditional isothermal models are not adequate in such situation. More recent works account for thermal effects and show that these interactions can be modeled in a thermodynamic consistent way (see [7]).

Another important pool of applications stems from biology, namely, modeling ion channels. Such channels are formed by charged walls and play a fundamental role in controlling and regulating the nervous system. In addition to the three main types of ion channels: voltage gated, ligand gated and chemically gated ion channels, temperature controlled ion channels are also been found and studied in the literature (see [8,9]). For example, six members of the mammalian Transient receptor potential ion channels (TRP) respond to varied temperature thresholds. TRPV1, TRPV2, TRPV3, and TRPV4 are heat activated, whereas TRPM8 and TRPA1 are activated by cold [9].

☆ The work of L. Zikatanov was supported in part by NSF grants DMS-1720114 and DMS-1819157.
* Corresponding author.
E-mail addresses: szw184@psu.edu (S. Wu), cliu124@iit.edu (C. Liu), ludmil@psu.edu (L. Zikatanov).

https://doi.org/10.1016/j.jcp.2020.109889
0021-9991/

Despite there is vast amount of works devoted on related experimental studies [6,2], mathematical modeling [10,11] and simulation [12], [13], thermodynamically consistent models are much less studied and developed.

To begin the discussion of the non-isothermal model we first consider the isothermal case and the Poisson-Nernst-Planck (PNP) system. This model is widely used to describe the transport of charged particles [14–17] with low concentration and couples the well-known drift-diffusion equations for the concentration with the Poisson equation for the electrostatic potential with appropriate initial and boundary conditions [18]:

$$-\nabla\cdot(\epsilon\nabla\phi) = e_c\sum_{i=1}^{N} q_i\rho_i, \qquad \text{(Poisson Equation)}$$

$$\frac{\partial\rho_i}{\partial t} = -\nabla\cdot\vec{J}_i, \qquad \text{(Drift Diffusion equation)}$$

$$\vec{J}_i = -D_i\nabla\rho_i - q_i\mu_i\rho_i\nabla\phi. \qquad \text{(Flux)}$$

Here ϵ is the dielectric constant, $D_i > 0$ is the diffusivity, q_i is the valence number, and μ_i is the mobility of the i-th ion species. The PNP system models the interaction of N ionic species through an electrostatic field, usually $N \geq 2$. ϕ is the electrostatic potential, ρ_i stands for the charge density of the i-th species.

Both ion channels and electroosmosis can be modeled by taking the background fluid into consideration and coupling the PNP system with the Navier-Stokes equation. The energetic variational formulation which deals with the isotropic case for the resulting system from a mechanical prospective is well elaborated in [19,20]. The energy law for this system, as stated in [19] is:

$$\frac{d}{dt}\{\int_{\Omega}\frac{1}{2}\rho_f|\vec{u}|^2 + \sum_{i=1}^{N}\rho_i(\rho_i-1) + \frac{\epsilon}{2}|\nabla\phi|^2 dx + \int_{\Gamma_R}\frac{\kappa}{2}|\phi|^2 ds\}$$
$$= -\int_{\Omega}\frac{\mu}{2}|\frac{\nabla\vec{u}+\nabla\vec{u}^T}{2}|^2 + \sum_{i=1}^{N}D_i\rho_i|\nabla(\log\rho_i + q_i\phi)|^2 dx.$$

Here, Γ_R denotes the part of boundary where the Robin boundary condition: $\epsilon\nabla\phi\cdot\vec{n} + \kappa\phi = C$ is imposed. The total energy consists of the sum of the kinetic energy of the background fluid, the electro potential energy and the free energy of each of the species. The dissipation of the total free energy is driven by the viscosity and diffusion. This coupled system can be derived through energetic variational approach (EVA, introduced in [21]) and is as follows:

$$-\nabla\cdot(\epsilon\nabla\phi) = e_c\sum_{i=1}^{N} q_i\rho_i, \qquad \text{(Poisson equation)}$$

$$\frac{\partial\rho_i}{\partial t} = -\nabla\cdot\vec{J}_i, \qquad \text{(Drift diffusion equation)}$$

$$\vec{J}_i = -D_i\nabla\rho_i - q_i\mu_i\rho_i\nabla\phi - \rho_i\vec{u}, \qquad \text{(Flux)}$$

$$\rho_f(\vec{u}_t + \vec{u}\cdot\nabla\vec{u}) + \nabla p = \nabla\cdot\frac{\nabla\vec{u}+\nabla\vec{u}^T}{2} - \sum_{i=1}^{N} q_i\rho_i\nabla\phi, \qquad \text{(NS equation)}$$

$$\nabla\cdot\vec{u} = 0. \qquad \text{(Incompressibility)}$$

As is evident from the equations above, this model does not take temperature effect into consideration.

A number of numerical solution approaches for the PNP system and relevant mathematical models have been considered in the literature. For example, A. Flavell et al. (2014) [22] applied a conservative finite difference scheme which achieves second-order accuracy in both space and time and also conserves total concentration for each ion species. C. Liu et al. (2015) [23] used an energetically stable finite element method for the PNP-NS(Poisson-Nernst-Planck-Navier-Stokes) system. In one of their follow-up paper [33], they presented a more effective numerical approach. D. Xie et al. (2016) [24] used a non-local finite element method for the PB (Poisson-Boltzmann) equation to tackle the problem of solution singularity caused by point charge term.

In order to capture the temperature change [25], [26] considered a thermodynamic approach for incompressible Newtonian fluid coupled with temperature model. The resulting model is based on the first law and the second law of thermodynamics and in accordance with the Fourier's Law assumes that the internal energy is proportional to the temperature and the heat flux is proportional to the temperature gradient. The equation for the temperature is derived through energy conservation and the whole system satisfies the inequality constraint for entropy production and this is in agreement with the second law of thermodynamics.

Some works in biology [10], [11], take both temperature and electrokinetics into consideration by a simple coupling which adds electrokinetic force into the Navier-Stokes equation and use PNP or Poisson-Boltzmann to model the electric field. The temperature effects are incorporated by including the Joule heat force term into the heat equation. One issue with this model is that it is unclear what is the energy associated with this system, moreover, it is not evident whether the second law of thermodynamics is satisfied by the model.

In our study, we are using a more consistent model to capture the interactions mentioned above. According to first law of thermodynamics, heat and work can convert to each other, so it is natural to consider this energy interchange in order to derive the equation for the temperature. By the second law of thermodynamics, the conversion between heat transfer and work follows the rule that keeps the entropy increasing. We follow the ideas in [7] and add this as an inequality constraint for the system. As it turns out, maintaining such inequality constraints is also crucial for the stability of the discretized model. This motivated the choice of discretization and we have applied the Edge Average Finite Element (EAFE, see [27]) discretization, which satisfies the discrete maximum principle for the temperature. The discrete maximum principle turns out to be the key to numerical stability and one of the key results that we present is the energy estimate satisfied by the numerical model.

The paper is organized as follows. We introduce the Heat-PNP equations in section 2 and the corresponding energy law in section 3. In section 4 we propose our discretization and prove an energy estimate for the discretized Heat-PNP system. In section 4 some numerical experiments are provided to validate the stability of our numerical scheme. We also provide numerical tests which show consistency with qualitative phenomena observed experimentally [1].

2. The heat-PNP equations and their discretization

As it is well known [28] the PNP system is as follows:

$$\begin{cases} \frac{\partial}{\partial t}\rho_i = \nabla\cdot\left(D_i\left(\nabla\rho_i + \frac{z_i e}{k_B T}\rho_i\nabla\phi\right)\right), i = 1, ..., N, \\ \nabla\cdot(\epsilon\nabla\phi) = -\left(\rho_0 + \sum_{i=1}^{N} z_i e\rho_i\right). \end{cases} \tag{2.1}$$

We treat the evolution equations for ions' concentration as a system of continuity equations. After introducing the flux variable for each ion species, this system can be written as:

$$\begin{cases} \frac{\partial\rho_i}{\partial t} = -\nabla\cdot\vec{J}_i, \\ \vec{J}_i = -D_i\nabla\rho_i - \frac{z_i e}{k_B T}\rho_i\nabla\phi, \\ \nabla\cdot(\epsilon\nabla\phi) = -\left(\rho_0 + \sum_{i=1}^{N} z_i e\rho_i\right). \end{cases} \tag{2.2}$$

We use the same fashion to rewrite the PNP system with temperature throughout this paper.

We consider the temperature PNP system in $\Omega \subseteq \mathbb{R}^n, n = 2, 3$ without background fluid. According to [7], this system has the form:

$$\begin{cases} \frac{\partial}{\partial t}\rho_i + \nabla\cdot(\rho_i\vec{u}_i) = 0, i = 1, ..., N, \\ \nu_i\rho_i\vec{u}_i = -k_B\nabla(\rho_i T) - z_i e\rho_i\nabla\phi, i = 1, ..., N, \\ -\nabla\cdot\epsilon\nabla\phi = \sum_i \rho_i z_i e + \rho_f, \\ \left(\sum_{i=1}^{N} k_B C_i\rho_i\right)\frac{\partial T}{\partial t} + \left(\sum_{i=1}^{N} k_B C_i\rho_i\vec{u}_i\right)\cdot\nabla T + \left(\sum_{i=1}^{N} k_B\rho_i\nabla\cdot\vec{u}_i\right)T = \\ \nabla\cdot k\nabla T + \sum_{i=1}^{N}\nu_i\rho_i|\vec{u}_i|^2 + q. \end{cases} \tag{2.3}$$

Here, ϕ is the electrostatic potential, ρ_i stands for the charge density of the i-th species, T is the temperature function and $\vec{u}_i$ is the macroscopic velocity of the i-th species. All these variables are space time functions defined on $\Omega \times [0, T]$. $D_i > 0$, q_i, and μ_i are correspondingly the diffusivity constant, the valence number and the constant mobility of the i-th ion species.

2.1. Initial and boundary conditions

For the system (2.3), the initial conditions at $t = 0$ are

$$T(x,0) = T_0(x), \quad \rho_i(x,0) = \rho_{i,0}(x), \quad i = 1,\dots,N, \quad x \in \Omega.$$

The boundary conditions are of different types: We have homogeneous no-flux boundary conditions for each of the concentrations of ion species,

$$\rho_i \vec{u_i} \cdot \vec{n} = 0 \text{ on } \partial\Omega.$$

For the Poisson equation, we partition the boundary into disjoint parts: $\partial\Omega = \Gamma_D \cup \Gamma_N \cup \Gamma_R$

$$\begin{aligned} \phi &= \delta V \text{ on } \Gamma_D, \\ \epsilon\nabla\phi \cdot \vec{n} &= E \text{ on } \Gamma_N, \\ \epsilon\nabla\phi \cdot \vec{n} + \kappa\phi &= C \text{ on } \Gamma_R. \end{aligned}$$

For the temperature equation we have Dirichlet boundary conditions which, as we show later help us in deriving the discrete energy law.

$$T = \delta T \text{ on } \partial\Omega.$$

3. Energy of the heat-PNP system

According to [7], the Heat-PNP system satisfies simultaneously first and second energy laws of thermodynamics, which are:

$$\begin{cases} \dfrac{d}{dt}(U+K) = \displaystyle\int_\Omega \left(q + \sum_{i=0}^{N} \rho_i \frac{\partial\psi}{\partial t}\right) d\mathbf{r} + \int_{\partial\Omega} k\nabla T d\mathbf{r}, \\ \dfrac{d}{dt} S = \Delta + \displaystyle\int_\Omega \frac{q}{T} d\mathbf{r} + \int_{\partial\Omega} \frac{k\nabla T}{T} d\mathbf{r}. \end{cases} \tag{3.1}$$

These laws involve the internal energy functional U, the kinetic energy functional K of the system, and the entropy functional S of the whole system. In addition, ψ is the applied electric field, which, for simplicity, we assume to be independent of time in our system here.

More precisely, if we substitute the predefined entropy functional and entropy production functional for Heat PNP system we obtain:

$$\begin{cases} S = -\displaystyle\sum_{i=1}^{N} \int_\Omega k_B \rho_i (\log\rho_i - C_i \log T - C_i) dx, \\ \Delta = \displaystyle\sum_{i=1}^{N} \int_\Omega \frac{\nu_i \rho_i |\vec{u_i}|^2}{T} + \frac{1}{k} \left| \frac{k\nabla T}{T} \right|^2 dx. \end{cases} \tag{3.2}$$

Next, we use the divergence theorem to derive the second law for our system in terms of the unknown variables:

$$\frac{d}{dt} \sum_{i=1}^{N} \int_\Omega k_B \rho_i (\log\rho_i - C_i \log T - C_i) dx = -\sum_{i=1}^{N} \int_\Omega \frac{\nu_i \rho_i |\vec{u_i}|^2}{T} + \frac{1}{k} |\frac{k\nabla T}{T}|^2 - \nabla \cdot (\frac{k\nabla T}{T}) dx. \tag{3.3}$$

In fact, to derive the second energy law of thermodynamics from the equation set is straightforward. We multiply by $\frac{1}{T}$ both sides of the heat equation (2.3) and integrate over the domain. For the left hand side we then we have

$$\begin{aligned} &\int_\Omega \sum_{i=1}^{N} k_B C_i \rho_i \frac{\partial T}{\partial t} \cdot \frac{1}{T} + \sum_{i=1}^{N} k_B C_i \rho_i \nabla \cdot (u_i T) \cdot \frac{1}{T} + \sum_{i=1}^{N} k_B (1 - C_i)(\rho_i) \nabla \cdot u_i dx \\ &= \int_\Omega \sum_{i=1}^{N} k_B C_i \rho_i \frac{\partial \log T}{\partial t} + \int_\Omega \sum_{i=1}^{N} k_B C_i (\frac{\nabla(\rho_i u_i T)}{T} - u_i \nabla \rho_i) + \sum_{i=1}^{N} k_B (1 - C_i)(\nabla(\rho_i u_i - u_i \nabla \rho_i)) dx \end{aligned}$$

$$= \int_\Omega \sum_{i=1}^N k_B C_i \rho_i \frac{\partial \log T}{\partial t} + \int_\Omega \sum_{i=1}^N k_B C_i (\nabla(\rho_i u_i) - \rho_i u_i \frac{\nabla T}{T} - u_i \nabla \rho_i) + \sum_{i=1}^N k_B (1 - C_i)(\frac{\rho_i}{\partial t} - \frac{\rho_i}{\partial t} \log \rho_i) dx$$

$$= \int_\Omega \sum_{i=1}^N k_B C_i \rho_i \frac{\partial \log T}{\partial t} + \int_\Omega \sum_{i=1}^N k_B C_i (-\frac{\rho_i}{\partial t} + \frac{\rho_i}{\partial t} \log T - -\frac{\rho_i}{\partial t} \log \rho_i) + \sum_{i=1}^N k_B (1 - C_i)(\frac{\rho_i}{\partial t} - \frac{\rho_i}{\partial t} \log \rho_i) dx$$

$$= \frac{d}{dt} \sum_{i=1}^N \int_\Omega k_B \rho_i (\log \rho_i - C_i \log T - C_i) dx.$$

Next, for the right hand side we have:

$$\int_\Omega \frac{\nabla \cdot k \nabla T}{T} + \sum_{i=1}^N \frac{\nu_i \rho_i |u_i|^2}{T} + \frac{q}{T} dx$$

$$= - \sum_{i=1}^N \int_\Omega \frac{\nu_i \rho_i |u_i|^2}{T} + \frac{1}{k} |\frac{k \nabla T}{T}|^2 - \nabla \cdot (\frac{k \nabla T}{T}).$$

Notice that in the derivation we used the continuity equations. Also, since this energy law is for closed systems, zero flux boundary condition is used when integrating by parts and finally we used that the heat source vanishes, namely, we have $q = 0$.

Clearly, the energy law (3.3) makes sense when ion concentrations and temperature are positive and the solution satisfies the following regularity assumptions:

$$\phi \in \mathbb{H}^1_{\Gamma_D} \equiv \{\nu \in \mathbb{H}^1(\Omega) |\ \nu|_{\Gamma_D} = \delta V\},$$
$$\rho_i \in W \equiv \mathbb{H}^1 \cap \mathbb{L}^\infty(\Omega)$$

3.1. Log-density formulation and its energy

We introduce a change of variables (also known as a log transformation for the ion concentrations) which is as follows

$$\eta_i(x,t) = \log \rho_i(x,t), i = 1, ..., N,$$
$$\xi(x,t) = \log T(x,t).$$

We note that such change of variables requires that the concentrations are positive and we have

$$\eta_i = \log \rho_i \in W \equiv \mathbb{H}^1 \cap \mathbb{L}^\infty(\Omega) \hookrightarrow \mathbb{H}^2$$

The embedding above holds for space dimensions $d \leq 3$. The Heat-PNP system then is written in a variational (weak) form: Find $\eta_i(t) \in W$, $\xi(t) \in W$ and $\phi \in \mathbb{H}^1_{\Gamma_D}$ such that:

$$\begin{cases} (\epsilon \nabla \phi, \nabla v) + \langle \kappa \phi, v \rangle_{\Gamma_R} - \sum_{i=1}^N q_i (e^{\eta_i}, v) = \langle C, v \rangle_{\Gamma_R} + \langle S, v \rangle_{\Gamma_N}, \\ (\frac{\partial}{\partial t} e^{\eta_i}, w) + (\frac{\nabla(e^{\eta_i} e^{\xi}) + e^{\eta_i} z_i e \nabla \phi}{\nu_i}, \nabla w) = 0, \\ (\sum_{i=1}^N k_B C_i e^{\eta_i} \frac{\partial}{\partial t} e^{\xi}, w) - (\sum_{i=1}^N k_B C_i e^{\xi} u_i, \nabla(e^{\eta_i} w)) + (k \nabla e^{\xi}, \nabla w) = (\sum_{i=1}^N \nu_i e^{\eta_i} |u_i|^2, w). \end{cases} \tag{3.4}$$

Here we denote by $\vec{u}_i$ the macroscopic velocity of i-th species defined as $\vec{u}_i = \frac{\nabla(e^{\eta_i} e^{\xi}) + e^{\eta_i} z_i e \nabla \phi}{\nu_i e^{\eta_i}}$, and for the energy law (3.3) we have

$$\frac{d}{dt} \sum_{i=1}^N \int_\Omega k_B e_i^\eta (\eta_i - C_i \xi - C_i) dx = - \sum_{i=1}^N \int_\Omega \frac{\nu_i e^{\eta_i} |u_i|^2}{T} + \frac{1}{k} |\frac{k \nabla T}{T}|^2 - \nabla \cdot (\frac{k \nabla T}{T}). \tag{3.5}$$

Furthermore, if we denote $\nu_i = 1$, $C_i = 1$, $z_i = 1$ and for simplicity we ignore the constant k_B, and under the appropriate zero flux boundary condition we arrive at the following simplified form of (3.3):

$$\frac{d}{dt}\sum_{i=1}^{N}\int_{\Omega} e_i^{\eta}(\eta_i-\xi-1)dx=-\sum_{i=1}^{N}\int_{\Omega}\frac{e^{\eta_i}|u_i|^2}{e^{\xi}}+k|\nabla\xi^2|. \tag{3.6}$$

The derivation of the energy law (3.6) from the variational form (3.4) is as follows: We choose the test function to be $e^{-\xi}$ in the temperature equation and we obtain

$$(\sum_{i=1}^{N}e^{\eta_i}\frac{\partial}{\partial t}e^{\xi},e^{-\xi})-(\sum_{i=1}^{N}e^{\xi}u_i,\nabla(e^{\eta_i}e^{-\xi}))+(k\nabla e^{\xi},\nabla e^{-\xi})=(\sum_{i=1}^{N}e^{\eta_i}|u_i|^2,e^{-\xi})$$

$$\int_{\Omega}\sum_{i=1}^{N}e^{\eta_i}\frac{\partial\xi}{\partial t}-(e^{\xi}(\nabla\eta_i+\nabla\xi)+z_ie\phi,e^{-\xi}e_i^{\eta}(\nabla\eta_i-\nabla\xi))-k|\nabla\xi^2|=\sum_{i=1}^{N}\int_{\Omega}\frac{e^{\eta_i}|u_i|^2}{e^{\xi}}$$

$$\int_{\Omega}\sum_{i=1}^{N}e^{\eta_i}\frac{\partial\xi}{\partial t}-(e^{\xi}e_i^{\eta}(\nabla\eta_i+\nabla\xi)+ez_ie_i^{\eta}\phi,(\nabla\eta_i-\nabla\xi))-k|\nabla\xi^2|=\sum_{i=1}^{N}\int_{\Omega}\frac{e^{\eta_i}|u_i|^2}{e^{\xi}}$$

Next, we test the continuity equation with $w=\eta_i-\xi$:

$$(\frac{\partial}{\partial t}e^{\eta_i},\eta_i-\xi)+(\nabla(e^{\eta_i}e^{\xi})+e^{\eta_i}z_ie\phi,\nabla(\eta_i-\xi))=0$$

$$(e^{\eta_i}\frac{\partial}{\partial t}\eta_i,\eta_i-\xi)=-(e^{\eta_i}e^{\xi}\nabla(\eta_i+\xi)+e^{\eta_i}z_ie\phi,\nabla(\eta_i-\xi))$$

Combining the temperature and the continuity equations together shows that:

$$\int_{\Omega}\sum_{i=1}^{N}e^{\eta_i}\frac{\partial\xi}{\partial t}+(e^{\eta_i}\frac{\partial}{\partial t}\eta_i,\eta_i-\xi)=-\sum_{i=1}^{N}\int_{\Omega}\frac{e^{\eta_i}|u_i|^2}{e^{\xi}}+k|\nabla\xi^2|$$

$$\int_{\Omega}\sum_{i=1}^{N}\frac{d}{dt}e^{\eta_i}(\eta_i-\xi-1)=-\sum_{i=1}^{N}\int_{\Omega}\frac{e^{\eta_i}|u_i|^2}{e^{\xi}}+k|\nabla\xi^2|$$

3.2. The discrete formulation

We consider a mesh $\mathbb{T}_h$ of simplices covering our computational domain (triangles in 2D or tetrahedra in 3D). As approximating space we take the space for piecewise linear, with respect to $\mathbb{T}_h$, continuous polynomials [29],

$$W_h\equiv\{w_h\in\mathbb{H}^1|w_h|_{\tau}\in\mathbb{P}^1\text{ for all }\tau\text{ in }\mathbb{T}_h\}\subset\mathbb{H}^1,$$
$$V_{g,\Gamma_D}\equiv\{v_h\in W_h|v|_{\Gamma_D}=g|_{\Gamma_D}.\}$$

The finite element solution to the Heat-PNP system then is defined using these finite element spaces. As a time marching scheme we choose the backward Euler scheme which is implicit and therefore stable. The discrete variational form then is: Find $\eta_{i,h}^j\in W_h,\xi_h^j\in W_h$ and $\phi_h^j\in V_{h,\Gamma_D}$

$$\begin{cases}(\epsilon\nabla\phi_h^j,\nabla v_h)+\langle\kappa\phi_h^j,v_h\rangle_{\Gamma_R}-\sum_{i=1}^{N}q_i(e^{\eta_{i,h}^j},v_h)=\langle C,v_h\rangle_{\Gamma_R}+\langle S,v_h\rangle_{\Gamma_N},\\ \frac{1}{\Delta t_j}(e^{\eta_{i,h}^j},w_h)+(\frac{\nabla(e^{\eta_{i,h}^j}e^{\xi_h^j}+q_i\phi_h^j)}{\nu_i},\nabla w_h)=\frac{1}{\Delta t_j}(e^{\eta_{i,h}^{j-1}},w_h),\\ \frac{1}{\Delta t_j}(\sum_{i=1}^{N}k_BC_ie^{\eta_{i,h}^j}e^{\xi_h^j}\xi_h^j,w_h)-(\sum_{i=1}^{N}k_BC_ie^{\xi_h^j}u_{i,h}^j,\nabla(\eta_{i,h}^j,w_h))+(k\nabla e^{\xi_h^j},\nabla w_h)=(\sum_{i=1}^{N}\nu_ie^{\eta_{i,h}^j}|u_{i,h}^j|^2,w_h)+\\ \frac{1}{\Delta t_j}(\sum_{i=1}^{N}k_BC_ie^{\eta_{i,h}^{j-1}}e^{\xi_h^j}\xi_h^{j-1},w_h).\end{cases} \tag{3.7}$$

The approximation to the initial conditions uses the standard interpolation operator I_h and is as follows:

$$\eta_i(x,0)=I_h(\log(\rho_{i,0}(x)))\text{ for x }\in\Omega,\text{ i = 1,...,N},$$
$$\xi(x,0)=I_h(\log(T_0(x)))\text{ for x }\in\Omega.$$

3.3. A discrete energy estimate

Next result shows a discrete energy estimate which holds in case when the mesh is quasi-uniform mesh and the stiffness matrix on each Picard iteration is an M-matrix. In this case, we can show that the corresponding discrete solution T_h^j satisfies maximum principle and with this condition satisfied, we have discrete energy estimate and mass conservation.

Theorem 1. *Suppose $\eta_{i,h}^j \in W_h$ and $\phi_h^j \in V_{h,\Gamma_D}$ satisfy equations (3.7) for $i = 1, .., N$ and the assumptions for the discrete maximum principle of temperature equation are satisfied. Then the mass is conserved for each ion species*

$$\int_\Omega e^{\eta_{i,h}^j(x,t)} dx = \int_\Omega e^{\eta_{i,h}^0(x,t)} dx, \text{ for } i = 1, .., N, \ j = 1, ...m. \tag{3.8}$$

Moreover, the discrete analogue of the energy estimate (second law of thermodynamics) holds

$$\begin{aligned}
&\sum_{i=1}^N \int_\Omega e^{\eta_{i,h}^j} (\eta_{i,h}^j - \xi_h^j - 1) dx \\
&\quad + \sum_{j=1}^m \Delta t_j \sum_{i=1}^N \int_\Omega - \frac{e^{\eta_{i,h}^j} |u_i|^2}{e^{\xi_h^j}} + |k \nabla e^{\xi_h^j}|^2 \cdot (1 + M h^{\frac{1}{2}}) \\
&\leq \sum_{i=1}^N \int_\Omega e^{\eta_{i,h}^0} (\eta_{i,h}^0 - \xi_h^0 - 1) dx,
\end{aligned}$$

where $\| e^{-\xi_h^j} \|_{W^{2,\infty}} \leq M$ and h is the mesh size.

Proof. For simplicity, let $\nu_i = 1$, $C_i = 1$, $z_i = 1$, $q = 1$, and $k_B = 1$, and the corresponding discrete energy estimate is done as follows. First, we choose $w_h \equiv 1 \in W_h$ in the first equation of (3.7) and this gives us:

$$\frac{1}{\Delta t_j} \int_\Omega e^{\eta_{i,h}^j} - e^{\eta_{i,h}^{j-1}} = 0.$$

For the energy estimate, we test the last equation in (3.7) with $w_h = I_h(e^{-\xi_{i,h}^j}) \in W_h$. The latter is a valid test function because $-\xi_{i,h}^j \in W_h$ and I_h is the interpolation operator mapping to the piecewise linear, continuous W_h. This gives us:

$$\begin{aligned}
&\underbrace{\frac{1}{\Delta t_j} \left(\sum_{i=1}^N e^{\eta_{i,h}^{j+1}} e^{\xi_h^j} \xi_h^{j+1}, I_h(e^{-\xi_h^j}) \right) - \frac{1}{\Delta t_j} \left(\sum_{i=1}^N e^{\eta_{i,h}^j} e^{\xi_h^j} \xi_h^j, I_h(e^{-\xi_h^j}) \right)}_{\text{I}} \\
&\underbrace{- (\sum_{i=1}^N e^{\xi_h^j} u_{i,h}^j, \nabla (e^{\eta_{i,h}^j} I_h(e^{-\xi_h^j})))}_{\text{II}} \\
&\underbrace{+ (k \nabla e^{\xi_h^j}, \nabla I_h(e^{-\xi_h^j}))}_{\text{III}} \\
&\underbrace{= (\sum_{i=1}^N \nu_i e^{\eta_{i,h}^j} |u_{i,h}^j|^2, \frac{1}{e^{\xi_h^j}})}_{\text{IV}}
\end{aligned}$$

We analyze each term in the above equation sum and we begin by rewriting I on the left hand side. We have

$$\begin{aligned}
\text{I} &= \frac{1}{\Delta t_j} (\sum_{i=1}^N e^{\eta_{i,h}^{j+1}} e^{\xi_h^j} \xi_h^{j+1}, I_h(e^{-\xi_h^j})) - \frac{1}{\Delta t_j} (\sum_{i=1}^N e^{\eta_{i,h}^j} e^{\xi_h^j} \xi_h^j, I_h(e^{-\xi_h^j})) \\
&= \frac{1}{\Delta t_j} ((\sum_{i=1}^N e^{\eta_{i,h}^{j+1}}, \xi_h^{j+1}) - (\sum_{i=1}^N e^{\eta_{i,h}^j}, \xi_h^j))(I_h(e^{-\xi_h^j}) e^{\xi_h^j}).
\end{aligned}$$

Next, we rewrite also II using integration by parts and the zero flux boundary conditions:

$$\begin{aligned}
\mathrm{II} &= -(\sum_{i=1}^{N} e^{\xi_h^j} u_{i,h}^j, \nabla(e^{\eta_{i,h}^j} I_h(e^{-\xi_h^j})))\\
&= (\sum_{i=1}^{N} \nabla(e^{\xi_h^j} u_{i,h}^j) e^{\eta_{i,h}^j} I_h(e^{-\xi_h^j}))\\
&= (I_h(e^{-\xi_h^j}) e^{\xi_h^j}) \cdot ((\sum_{i=1}^{N} u_{i,h}^j e^{\eta_{i,h}^j}, \nabla \xi_h^j) + (\sum_{i=1}^{N} \nabla u_{i,h}^j e^{\eta_{i,h}^j}, 1))\\
&= (I_h(e^{-\xi_h^j}) e^{\xi_h^j}) \cdot (\frac{1}{\Delta t_j}(e^{\eta_{i,h}^{j+1}}, \eta_{i,h}^{j+1} - \xi_h^j - 1) - \frac{1}{\Delta t_j}(e^{\eta_{i,h}^j}, \eta_{i,h}^j - \xi_h^j - 1)).
\end{aligned}$$

In the last step we used the discretized continuity equation to estimate term III on the left hand side as follows:

$$\begin{aligned}
\mathrm{III} &= (k\nabla e^{\xi_h^j}, \nabla I_h(e^{-\xi_h^j}))\\
&= k|\nabla e^{\xi_h^j}|^2 - (k\nabla e^{\xi_h^j}, \nabla I_h(e^{-\xi_h^j}) - \nabla e^{-\xi_h^j})\\
&\le k|\nabla e^{\xi_h^j}|^2 + k\|\nabla e^{\xi_h^j}\|_2 \cdot \|\nabla I_h(e^{-\xi_h^j}) - \nabla e^{-\xi_h^j}\|_2.
\end{aligned}$$

Here we have used the assumption that $e^{-\xi^j} \in W^{2,\infty}$, $e^{-\xi_h^j} \in W^{2,\infty}$ for any j. Also, these constants are uniformly bounded by the constant M. As shown in [30, Theorem 3.1.6] we have the following interpolation estimate

$$\|\nabla I_h(e^{-\xi_h^j}) - \nabla e^{-\xi_h^j}\|_{L^2} \le Ch|e^{-\xi_h^j}|_{2,\Omega} = C(\Omega)hM.$$

Term IV on the right hand side:

$$\left(\sum_{i=1}^{N} \nu_i e^{\eta_{i,h}^j} |u_{i,h}^j|^2, \frac{1}{e^{\xi_h^j}}\right) = \left(\frac{\sum_{i=1}^{N} \nu_i e^{\eta_{i,h}^j} |u_{i,h}^j|^2}{e^{\xi_h^j}}\right) (I_h(e^{-\xi_h^j}) e^{\xi_h^j}).$$

Combining all the terms above and by a discrete Grønwall argument of telescopic sum from time step t=0 to m and, as a result, we obtain the following energy estimate:

$$\sum_{j=1}^{m} \Delta t_j \,(\mathrm{I} + \mathrm{II}) \ge \sum_{j=1}^{m} \Delta t_j \left(\mathrm{IV} - (Ch|I_h(e^{-\xi_h^j}) - e^{-\xi_h^j}|_{2,\Omega} \cdot \|\nabla e^{\xi_h^j}\|_2)\right),$$

only keep the term $\sum_{i=1}^{N} \int_\Omega e^{\eta_{i,h}^0}(\eta_{i,h}^0 - \xi_h^0 - 1)dx$ in I to the right side, we have:

$$\begin{aligned}
&\sum_{i=1}^{N} \int_\Omega e^{\eta_{i,h}^j}(\eta_{i,h}^j - \xi_h^j - 1)dx\\
&+ \sum_{j=1}^{m} \Delta t_j \sum_{i=1}^{N} \int_\Omega -\frac{e^{\eta_{i,h}^j}|u_i|^2}{e^{\xi_h^j}} + |k\nabla e^{\xi_h^j}|^2 \cdot (\frac{1}{(I_h(e^{-\xi_h^j}) e^{\xi_h^j})})\\
&+ \frac{1}{(I_h(e^{-\xi_h^j}) e^{\xi_h^j})} \cdot (Ch|I_h(e^{-\xi_h^j}) - e^{-\xi_h^j}|_{2,\Omega} \cdot \|\nabla e^{\xi_h^j}\|_2)dx\\
&\le \sum_{i=1}^{N} \int_\Omega e^{\eta_{i,h}^0}(\eta_{i,h}^0 - \xi_h^0 - 1)dx,
\end{aligned}$$

divide the equation by $I_h(e^{-\xi_h^j}) e^{\xi_h^j}$ on both sides, use $I_h(e^{-\xi_h^j}) e^{\xi_h^j} \ge 1$ and notice I_h is a piecewise linear interpolant of a convex (the exponential) function shows that we can drop the term $I_h(e^{-\xi_h^j}) e^{\xi_h^j}$ from the equation above and obtain the final estimate:

$$\sum_{i=1}^{N}\int_{\Omega} e^{\eta_{i,h}^{j}}(\eta_{i,h}^{j}-\xi_h^{j}-1)dx$$
$$+\sum_{j=1}^{m}\Delta t_j\sum_{i=1}^{N}\int_{\Omega}-\frac{e^{\eta_{i,h}^{j}}|u_i|^2}{e^{\xi_h^{j}}}+|k\nabla e^{\xi_h^{j}}|^2\cdot(\frac{1+ChM}{(I_h(e^{-\xi_h^{j}})e^{\xi_h^{j}})})dx$$
$$\leq\sum_{i=1}^{N}\int_{\Omega} e^{\eta_{i,h}^{0}}(\eta_{i,h}^{0}-\xi_h^{0}-1)dx.\quad\square$$

In order to show that our numerical model meets the criteria of Theorem 1, we need to show that the discrete solution for the nonlinear temperature equation has an L^2 norm which is bounded below, uniformly with respect to time. To see this, observe that on each time step, we are solving a nonlinear drift diffusion equation for the temperature. We linearize these equations using a Picard iteration. The solutions to the Picard iteration satisfy the discrete maximum principle because we used EAFE discretization for the linearized equations.

3.4. Fixed-point iteration

We next write out the Picard iteration algorithm for the temperature equation which we solve each time step.

Algorithm 1 Fixed Point Iteration for temperature equation.

for j = 1,2,3,...T **do** ▷ time iteration
  Get the solution from last time step: $\xi_h^{j-1}, \eta_{i,h}^{j-1}, \phi_h^{j-1}$;
  Choose a small number ϵ and set $\xi^0=\xi_h^{i-1}$
  for k = 1,2,3,...maxiter **do** ▷ Non-linear Picard iteration:
    Solve the linearized concentration equation and the Poisson equation using the temperature term from last nonlinear iteration step ξ^{k-1};
    Solve the linearized equation for temperature with the given Dirichlet boundary condition
    if $\|\xi^k-\xi^{k-1}\|_2\leq\epsilon$ **and** $\|\eta_i^k-\eta_i^{k-1}\|_2\leq\epsilon$ for all i **then** ▷ Convergence Criteria
      Stop
    else
      k=k+1

Here, the linearized concentration equations are:

$$\frac{1}{\Delta t_j}(e^{\eta_{i,h}^{j,k}},w_h)+(\frac{\nabla(e^{\eta_{i,h}^{j,k}}e^{\xi_h^{j,k-1}}+q_i\phi_h^{j,k-1})}{\nu_i},\nabla w_h)=\frac{1}{\Delta t_j}(e^{\eta_{i,h}^{j-1}},w_h)\text{ for i = 1,2,...N.}$$

The linearized temperature equation is:

$$\frac{1}{\Delta t_j}(\sum_{i=1}^{N}k_BC_ie^{\eta_{i,h}^{j}}e^{\xi_h^{j,k}},w_h)-(\sum_{i=1}^{N}k_BC_ie^{\xi_h^{j}}u_{i,h,k-1}^{j},\nabla(\eta_{i,h}^{j},w_h))+(k\nabla e^{\xi_h^{j}},\nabla w_h)$$
$$=(\sum_{i=1}^{N}\nu_ie^{\eta_{i,h}^{j}}|u_{i,h,k-1}^{j}|^2,w_h)+\frac{1}{\Delta t_j}(\sum_{i=1}^{N}k_BC_ie^{\eta_{i,h}^{j-1}}e^{\xi_h^{j-1}},w_h),$$

here, $u_{i,h,k-1}^{j}$ has the meaning of we use the temperature from $(k-1)$-th fixed point iteration step to compute the discretized velocity term. The superscript k stands for the nonlinear iteration step.

3.5. Discrete maximum principle with EAFE stabilization

For the sake of clarity, we change the variables back and use the original density and temperature variable. It is easy to see that the corresponding continuous temperature equation in each Picard iteration has this form:

$$\frac{1}{\Delta t}\left(\sum_{i=1}^{N}\rho_{i,h}^{j,k}\right)T_h^{j,k}+\left(\sum_{i=1}^{N}\rho_{i,h}^{j,k}\vec{u}_{i,h}^{j,k-1}\right)\cdot\nabla T_h^{j,k}+\left(\sum_{i=1}^{N}\rho_{i,h}^{j,k}\nabla\cdot\vec{u}_{i,h}^{j,k-1}\right)T_h^{j,k}$$
$$=\nabla\cdot k\nabla T_h^{j,k}+\sum_{i=1}^{N}\nu_i\rho_{i,h}^{j,k}|\vec{u}_{i,h}^{j,k}|^2+\frac{1}{\Delta t}\left(\sum_{i=1}^{N}\rho_{i,h}^{j,k}\right)T_h^{j,k-1}.$$

This can be written in a more concise form:

$$LT_h^{j,k} = \sum_{i=1}^{N} \nu_i \rho_{i,h}^{j,k} |\vec{u}_{i,h}^{j,k}|^2,$$

where the differential operator for the temperature equation:

$$Lu = -k \sum_{i,j=1}^{n} u_{x_i x_j} + \sum_{i=1}^{n} b^i u_{x_i} + cu,$$

and $c = \frac{1}{\Delta t} - \left(\sum_{i=1}^{N} \rho_{i,h}^{j,k} \nabla \cdot \vec{u}_{i,h}^{j,k-1}\right)$, $b^i = \left(\sum_{i=1}^{N} \rho_{i,h}^{j,k} \vec{u}_{i,h}^{j,k-1}\right)^i$. It is crucial that the time step is chosen so that the parameter c in front of the temperature term is always positive because this implies that the linearized differential operator is uniformly elliptic. Also the right hand side is always positive, and hence,

$$LT_h^{j,k} \geq 0 \text{ in } \Omega.$$

If we assume that the linearized temperature equation has a classical solution in $C^2(\Omega) \cap C(\bar{\Omega})$, according to [31] our solution satisfies weak maximum principle [31] and the minimum of the temperature must be attained at the boundary. In applications this Dirichlet boundary condition is always positive which implies that we have a uniform upper bound on $\|T_h^j\|_2$ for all time steps.

In order to meet the criteria for the discrete energy estimate in Theorem 1, the inverse of discretized temperature solution from the nonlinear solver at each time step needs to satisfy a global upper bound in the L^2 sense. This requires a special numerical treatment of the temperature equation. Inspired by techniques introduced in a recent work [23], we maintain a discrete maximum principle for the advection diffusion equation with source term in the following way: To do this we rewrite the linearized equations for temperature in divergence form and then use the EAFE scheme to guarantee that the discrete maximum principle is satisfied and the maximum of the temperature is on the boundary.

$$\nabla(-k\nabla T_h^{j,k} + \sum_{i=1}^{N} \rho_{i,h}^{j,k} \vec{u}_{i,h}^{j,k-1} T_h^{j,k}) + cT_h^{j,k} = G(\vec{u}_{i,h}^{j,k-1}, \rho_{i,h}^{j,k}, T_h^{j,k-1}). \tag{3.9}$$

Here, $c = c(\Delta t, \rho_{i,h}^{j,k}, \vec{u}_{i,h}^{j,k-1}) = \frac{1}{\Delta t} - \left(\sum_{i=1}^{N} \nabla \rho_{i,h}^{j,k} \vec{u}_{i,h}^{j,k-1}\right)$, and G is always positive. The corresponding weak form for the linearized equation is

$$(k\nabla T_h^{j,k} + \sum_{i=1}^{N} \rho_{i,h}^{j,k} \vec{u}_{i,h}^{j,k-1} T_h^{j,k}, \nabla w) + (cT_h^{j,k}, w) = (G(\vec{u}_{i,h}^{j,k-1}, \rho_{i,h}^{j,k}, T_h^{j,k-1}), w). \tag{3.10}$$

We apply mass lumping to the term $(cT_h^{j,k}, w)$, using nodal interpolant $I_h : W \to W_h$,

$$(cT_h^{j,k}, w)_h = \int_{\Omega} I_h((\frac{1}{\Delta t} - \left(\sum_{i=1}^{N} \nabla \rho_{i,h}^{j,k} \vec{u}_{i,h}^{j,k-1}\right)) T_h^{j,k}) I_h(w) dx,$$

and EAFE approximation to the flux term:

$$\begin{aligned} a_h(k\nabla T_h^{j,k} + \sum_{i=1}^{N} \rho_{i,h}^{j,k} \vec{u}_{i,h}^{j,k-1} T_h^{j,k}, w) &:= \sum_{\tau \in \mathbb{T}_h} \sum_{E \in \tau} \omega_E^{\tau} \frac{|E|}{\int_E e^{c(\Delta t, \rho_{i,h}^{j,k}, \vec{u}_{i,h}^{j,k-1}) ds}} \delta_E(e^{c(\Delta t, \rho_{i,h}^{j,k}, \vec{u}_{i,h}^{j,k-1})} T_h^{j,k}) \delta_E(w) \\ &\approx (k\nabla T_h^{j,k} + \sum_{i=1}^{N} \rho_{i,h}^{j,k} \vec{u}_{i,h}^{j,k-1} T_h^{j,k}, \nabla w). \end{aligned}$$

The changes in notation used above are summarized as follows:

- $\mathbb{T}_h$ is either the triangulation in 2d or tetrahedron in 3d.
- τ stands for the simplex.
- E stands for the edges.
- ω_E is the entries in the stiffness matrix for the Laplace equation.

The detailed derivation and proof of monotonicity as well as the restrictions on the mesh needed for such a proof are found in [27].

As a result we have the following theorem providing discrete energy estimate.

Theorem 2. *Suppose that the Dirichlet boundary condition for temperature is strictly positive and no-flux boundary condition is imposed for each ion density, then our nonlinear Picard iteration approach using EAFE scheme with appropriate small time step satisfies the discrete energy estimate:*

$$\begin{aligned}
&\sum_{i=1}^{N}\int_{\Omega} e^{\eta_{i,h}^{j}}(\eta_{i,h}^{j}-\xi_h^{j}-1)dx\\
&\quad+\sum_{j=1}^{m}\Delta t_j\sum_{i=1}^{N}\int_{\Omega}\frac{e^{\eta_{i,h}^{j}}|u_i|^2}{e^{\xi_h^{j}}}+|k\nabla e^{\xi_h^{j}}|^2\cdot(1+Mh^{\frac{1}{2}})dx\\
&\le\sum_{i=1}^{N}\int_{\Omega} e^{\eta_{i,h}^{0}}(\eta_{i,h}^{0}-\xi_h^{0}-1)dx,
\end{aligned}$$

where $\|e^{-\xi_h^{j}}\|_{W^{2,\infty}}\le M$ *and h is the mesh size, and also the conservation of charge is satisfied:*

$$\int_{\Omega} e^{\eta_{i,h}^{j}(x,t)}dx=\int_{\Omega} e^{\eta_{i,h}^{0}(x,t)}dx,\ \textit{for } i=1,..,N,\ j=1,...m. \tag{3.11}$$

4. Numerical experiments

The first numerical example is for the modeling of an electric device which consists of two kinds of ionic solutions: Na and Cl. We compute the current, density and temperature profile under given fixed Voltage and outside temperature. With initial condition $\rho_{\pm}(x,0)=\rho_0=0.06$ and $T(x,0)=1$. The dimensionless parameters are, $C_0\rho_0=302$, $C_{\pm}=3$, $1/\nu_+=1.334$, $1/\nu_-=2.032$ [32], $\epsilon=1$, $l_B=0.714$. In order to highlight the contribution from temperature, we choose a relatively small heat conductance $k=100$. The computational domain is $[0,10]\times[0,1]$. The boundary condition for ion density and temperature are Dirichlet, i.e. $\rho_i(0,t)=\rho_i(L,t)=\rho_0$, $T(0,t)=T(L,t)=1$.

4.1. Demonstrating discrete energy dissipation

Notice that we need zero boundary flux for each of the ion species in order to have charge (mass) conservation and discrete energy estimate. In the numerical experiment presented in this section we are imposing Dirichlet boundary conditions on ion densities, and our system is no longer a closed system. Thus, the energy estimate needs to take into consideration the boundary flux. In such setting, the exact conservation law of entropy is as follows:

$$\frac{d}{dt}S(V,t)+\int_{\partial V}\frac{j}{T}\cdot d\mathbf{r}-\int_{V}\frac{q}{T}d\mathbf{r}-J_S=\Delta(V,t)\ge 0. \tag{4.1}$$

The numerical results suggest that after a short time period the system tends to its equilibrium state and the bulk entropy is always increasing and tends to a limit. The entropy production cancels with the boundary flux of entropy when equilibrium is reached. This is exactly what we expected (see Fig. 4.1).

The steady state of PNP equation satisfies Poisson-Boltzmann (PB) equation. But we can not directly compare our steady state solution to PB solution since temperature effect is not considered there. To validate the accuracy of our numerical method, we observe similar steady-state solution with the PNP solution in previous work [7].

As is shown below, the temperature profile at steady-state is concave. On the other hand the charged densities are convex. With different increasing voltage by setting different electric potential on each side of the tube, the current I does not increase linearly as in the non-isothermal case. This is more accurate model as the increase in voltage changes the temperature and the device we model becomes a non-linear device (see Fig. 4.2).

4.2. Modeling electroosmosis flow

We consider two ionic species with incompressible background fluid in an rectangular shape tube. Then the dynamic equations for the solute particles become,

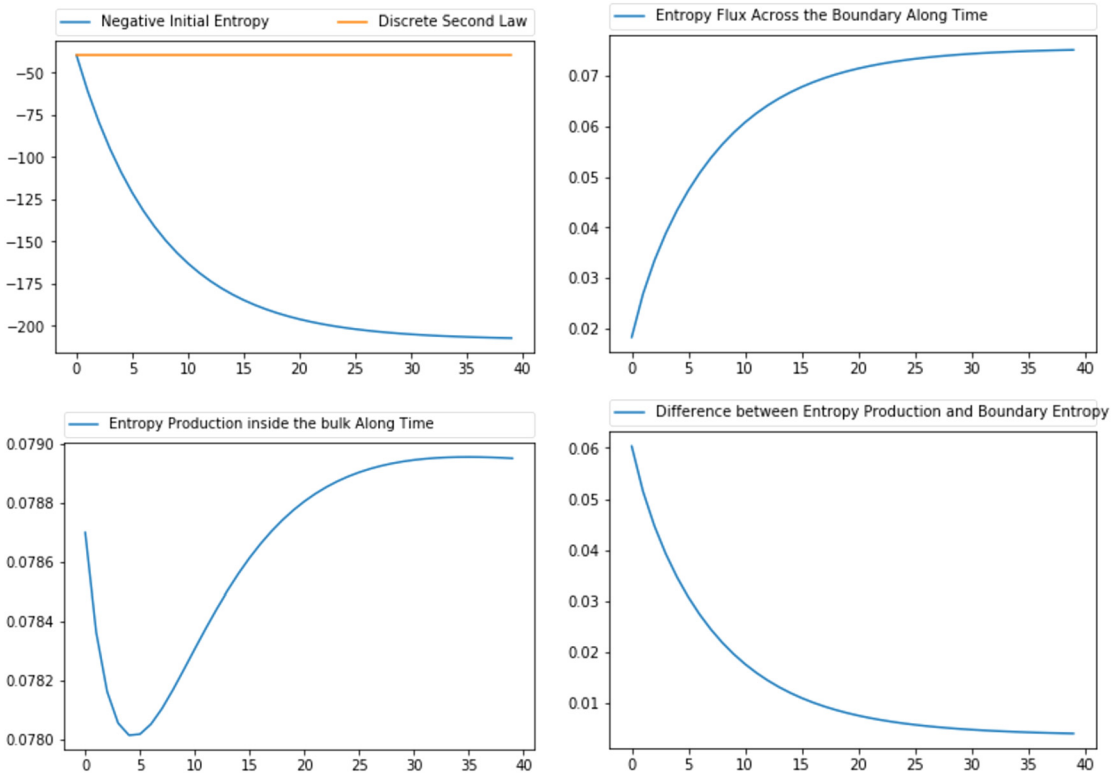

Fig. 4.1. When the system approaching to steady state. (a) Bulk Entropy is increasing and tends to a limit (b) Entropy Flux at the Boundary is decreasing to a limit (c) Dissipation is decreasing to a limit (d) The difference between Dissipation and Entropy Flux tends to zero. (For interpretation of the colors in the figure(s), the reader is referred to the web version of this article.)

$$\begin{cases} \dfrac{\partial}{\partial t}\rho_i + \nabla\cdot(\rho_i u_i) = 0, \\ m_i\rho_i(\dfrac{\partial u_i}{\partial t} + u_i\nabla u_i) + \nabla P_i + \rho_i z_i e\nabla\phi = \nu_i\rho_i(u_0 - u_i) + \nabla(\xi_i\nabla\cdot u_i) + \nabla\cdot\lambda_i\nabla u_i, \\ -\nabla\cdot\epsilon\nabla\phi = \sum_{m=1}^{N}\rho_m z_m e + \rho_f. \end{cases} \tag{4.2}$$

Where P_i is the thermodynamic pressure which we will be giving out later. Here we use the fact that $-\nabla\cdot\epsilon\nabla v(\mathbf{r},\mathbf{r}') = \delta(\mathbf{r}-\mathbf{r}')$, where ϵ is the dielectric constant. And $\rho_f = -\nabla\cdot\epsilon\nabla\psi$ describes the external field. For the incompressible solvent,

$$\begin{cases} m_0\rho_0\left(\dfrac{\partial}{\partial t}u_0 + u_0\nabla u_0\right) + \nabla P_0 + \rho_0\nabla\phi_0 = \displaystyle\sum_{i=1}^{N}\nu_i\rho_i(u_i - u_0) + \nabla\cdot\lambda_0\nabla u_0, \\ \nabla\cdot u_0 = 0. \end{cases} \tag{4.3}$$

And the temperature equation,

$$\begin{aligned} &\sum_{i=0}^{N}\left(-T\frac{\partial^2\Psi_i}{\partial T^2}\right)\left(\frac{\partial T}{\partial t} + u_i\cdot\nabla T\right) + \left(\sum_{i=1}^{N}\frac{\partial P_i}{\partial T}\nabla\cdot u_i\right)T \\ =&\nabla\cdot k\nabla T + \sum_{i=1}^{N}\nu_i\rho_i|u_i - u_0|^2 + \xi_i|\nabla\cdot u_i|^2 + \sum_{i=0}^{N}\lambda_i|\nabla u_i|^2 + q. \end{aligned} \tag{4.4}$$

In (4.4), the term $\sum_{i=0}^{N}\left(-T\frac{\partial^2\Psi_i}{\partial T^2}\right)$ can be viewed as the weighted average heat capacitance of the system. The second term represents the work of thermopressure transfer into heat. On the right hand side, $\nabla\cdot k\nabla T$ describes the heat diffusion. We notice that the entropy production from mechanical viscosity appears as an internal heat source.

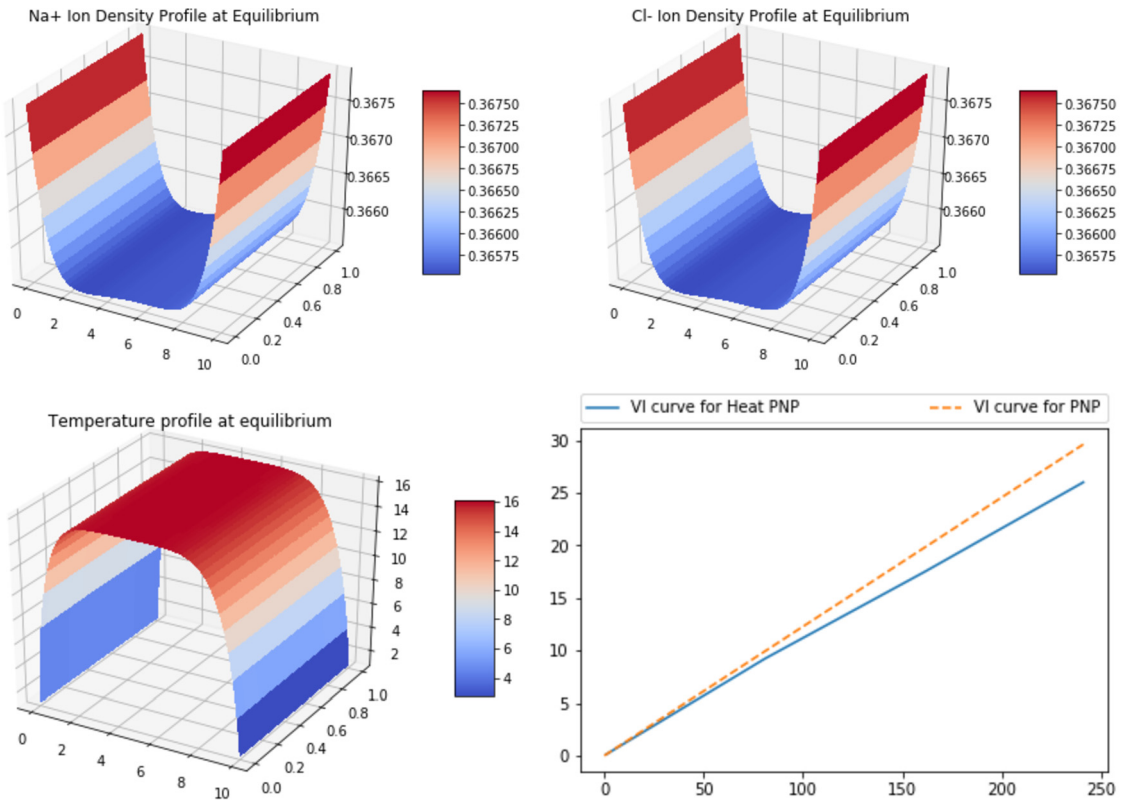

Fig. 4.2. When the system approaching to steady state. (a) Na^+ density distribution. (b) Cl^- density distribution. (c) Temperature distribution. (d) Voltage-Current relation of the system.

Following the notation of [7], the free energy of the whole system is:

$$F(V,t) = \int_\Omega \Psi_0(\rho_0(\mathbf{r},t), T(\mathbf{r},t)) + \Psi_1(\rho_1(\mathbf{r},t), T(\mathbf{r},t)) + \Psi_2(\rho_2(\mathbf{r},t), T(\mathbf{r},t))d\mathbf{r} \tag{4.5}$$

$$+ \sum_{i,m=0}^{N} \frac{z_i z_m e^2}{2} \int_V \int_\Omega \rho_i(\mathbf{r},t)\rho_m(\mathbf{r}',t)v(\mathbf{r},\mathbf{r}')d\mathbf{r}d\mathbf{r}'$$

$$+ \sum_{i=0}^{N} z_i e \int_V \rho_i(\mathbf{r})\psi(\mathbf{r},t)d\mathbf{r}. \tag{4.6}$$

Where:

$$\Psi_0(\rho_0(\mathbf{r},t), T(\mathbf{r},t)) = T(\mathbf{r})\log T(\mathbf{r}), \tag{4.7}$$

is the free energy term for the solvent.
Ψ_i, i = 1,2 which are the free energy terms for the two ionic species are given by:

$$\Psi_i(\rho_i(\mathbf{r},t), T(\mathbf{r},t)) = k_B T(\mathbf{r},t)\rho_i(\mathbf{r},t)\left[\log \rho_i(\mathbf{r},t) - C_i \log T(\mathbf{r},t)\right]. \tag{4.8}$$

The corresponding thermodynamic pressure will be:

$$\begin{cases} P_i = \rho_i T, i = 1,2 \\ P_0 = -T\log T, \end{cases} \tag{4.9}$$

and the whole system equations is as follows:

Table 4.1
Parameter values for the second numerical experiment.

Parameter List		
Parameter Name	Parameter Explanation	Value
$\phi\|_{x=0} - \phi\|_{x=10}$	Voltage	100
ρ	background fluid density	1
k	Heat conductance	100
Cv	Heat Capacitance	300
z	ASM	1
e	AND	1
μ	Mobility constant for background fluid	1
μ_1	Mobility constant for positive charge	1.334
μ_2	Mobility constant for positive charge	2.032
ϵ	Dielectric constant	1
q_1	positive charge valence number	1
q_2	negative charge valence number	-1

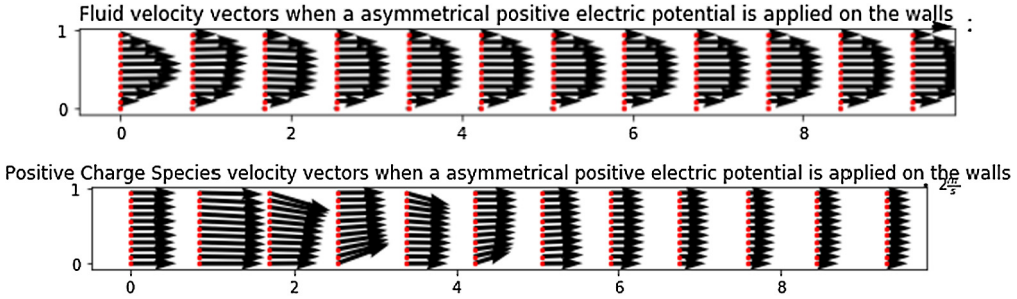

Fig. 4.3. Velocity plot of the positive charge species and the background fluid. (a) Background fluid velocity (b) Positive charge species velocity.

$$
\begin{cases}
\dfrac{\partial}{\partial t}\rho_i + \nabla\cdot(\rho_i\vec{u}_i) = 0, i = 0, 1, 2, \\
\nu_i\rho_i(\vec{u}_i - \vec{u}_0) = -k_B\nabla(\rho_i T) - z_i e\rho_i\nabla\phi, i = 1, 2, \\
m(\dfrac{\partial}{\partial t}\vec{u}_0 + \vec{u}_0\nabla\vec{u}_0) + \nabla P_0 + \displaystyle\sum_{i=1}^{2}\nu_i\rho_i(\vec{u}_0 - \vec{u}_i) = \nabla\cdot\lambda_0\nabla\vec{u}_0, \\
\nabla\cdot\vec{u}_0 = 0, \\
-\nabla\cdot\epsilon\nabla\phi = \displaystyle\sum_i \rho_i z_i e + \rho_f, \\
\left(\displaystyle\sum_{i=0}^{2} k_B C_i\rho_i\right)\dfrac{\partial T}{\partial t} + \left(\displaystyle\sum_{i=0}^{2} k_B C_i\rho_i\vec{u}_i\right)\cdot\nabla T + \left(\displaystyle\sum_{i=1}^{2} k_B\rho_i\nabla\cdot\vec{u}_i\right)T = \\
\nabla\cdot k\nabla T + \sum_{i=1}^{N}\nu_i\rho_i|\vec{u}_i - \vec{u}_0|^2 + \lambda_0|\vec{u}_0|^2 + q.
\end{cases}
$$

We first apply asymmetrical boundary zeta potentials along the upper and lower wall of the channel and list the parameter values in Table 4.1.

The velocity plot of the positive charge species and the background fluid are shown in Fig. 4.3.

Local Nusselt Number is used to describe the effect of zeta potentials on heat transfer which is defined by

$$Nu = \frac{-h\frac{\partial T}{\partial y}}{T_w - T_m}, \tag{4.10}$$

where h is the width of channel, T_w is the wall temperature, T_m is the bulk mean temperature, and y is the perpendicular distance from the channel walls. The Nusselt number along the upper and lower walls at stationary state is as shown in Fig. 4.4.

We can see the zeta potential will cause perpendicular uneven distribution of the temperature, thus may have negative effect on the horizontal charge transport efficiency and also may have negative effect on the charge separation.

We also computed the case where no zeta potential on the side walls are posed. In this case we examined the stationary temperature profile development and focusing on two aspects the radial and horizontal distribution.

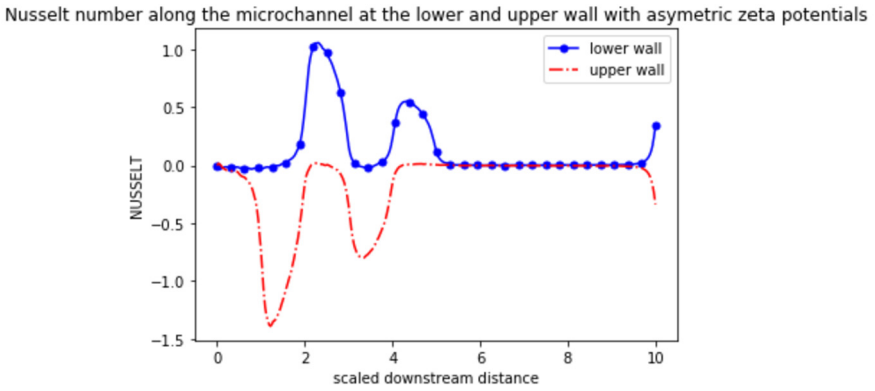

Fig. 4.4. Nusselt number along the upper and lower wall of channel.

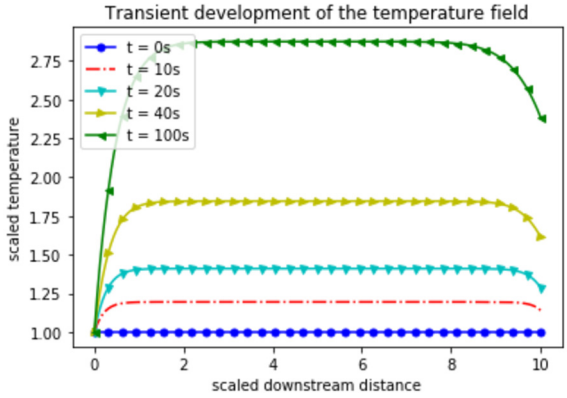

Fig. 4.5. The transient development of the temperature field.

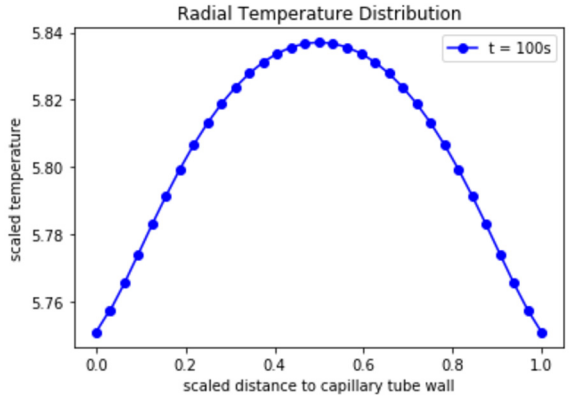

Fig. 4.6. Radial temperature profile at equilibrium at the midpoint of channel.

The above Fig. 4.5 shows the transient development of the temperature field. The Joule heating effect is explicitly showed as time goes on, the temperature of the whole capillary tube has been elevated. The plot shows the temperature profile in horizontal direction of the center, and the temperature gradients are mainly in the inlet and outlet.

Radial temperature profile has a parabola like shape, large radial temperature gradient may have negative effect on charge separation and electroosmosis process since the temperature gradient will induce charge motions orthogonal to axial direction (Fig. 4.6).

In our model we captured the effect of temperature distribution exhibiting a parabolic profile across the horizontal direction of the tube. But the main influence on separation efficiency is via the establishment of a radial temperature profile across the lumen of the channel. An overall increase in temperature of the background fluid has low influence on the overall quality of separation. It is known that Joule heating parameter, auto thermal Joule heating parameter, external

cooling parameter, Peclet number are crucial in the process of electroosmosis. Which can be translated into our model. Our full numerical experiment model will have the ability of using control variable on various parameter and boundary conditions to examine the effects from different factors on the quality of separation.

5. Conclusions

We proposed a general framework for solving Non-Isothermal electrokinetics equation based on a discretization using a logarithmic transformation of the charge carrier densities and temperature variable. We designed the numerical method for approximation of the nonlinear fixed point iteration so that it meets the sufficient conditions for strict discrete energy dissipation. The discrete energy estimate, inherited from the continuous case, is satisfied and this shows consistency of our numerical model with the thermodynamic laws. Introducing more complex computational domains and coupling with Navier Stokes equation allows for generalization of the numerical models to electrochemistry and electrophysiology to study the heat effect for battery, semiconductor and temperature gated ion channels. Such topics are in the focus of our current and future research.

CRediT authorship contribution statement

Simo Wu: Writing - original draft. **Chun Liu:** Supervision. **Ludmil Zikatanov:** Writing - review & editing.

Declaration of competing interest

The authors declare that they have no known competing financial interests or personal relationships that could have appeared to influence the work reported in this paper.

References

[1] P. Nithiarasu, P. Eng, A. Arnold, Flow and Heat Transfer in Micro-Channels-Electro-Osmotic Flow (eof), 05 2008.
[2] J.H. Knox, K.A. McCormack, Temperature effects in capillary electrophoresis. 1: internal capillary temperature and effect upon performance, Chromatographia 38 (Feb 1994) 207–214.
[3] M. Eleuteri, E. Rocca, G. Schimperna, On a non-isothermal diffuse interface model for two-phase flows of incompressible fluids, Discrete Contin. Dyn. Syst. 35 (6) (2015) 2497–2522.
[4] A. González, A. Ramos, H. Morgan, N.G. Green, A. Castellanos, Electrothermal flows generated by alternating and rotating electric fields in microsystems, J. Fluid Mech. 564 (2006) 415–433.
[5] S. Sanchez, J. Arcos, O. Bautista, F. Mendez, Joule heating effect on a purely electroosmotic flow of non-Newtonian fluids in a slit microchannel, J. Non-Newton. Fluid Mech. 192 (02 2013) 1–9.
[6] E. Grushka, R.M. McCormick, J.J. Kirkland, Effect of temperature gradients on the efficiency of capillary zone electrophoresis separations, Anal. Chem. 61 (02 1989) 241–246.
[7] P. Liu, S. Wu, C. Liu, Non-isothermal Electrokinetics: Energetic Variational Approach, 2017.
[8] P. Cesare, A. Moriondo, V. Vellani, P.A. McNaughton, Ion channels gated by heat, Proc. Natl. Acad. Sci. 96 (14) (1999) 7658–7663.
[9] D.S. Reubish, D.E. Emerling, J. DeFalco, D. Steiger, C.L. Victoria, F. Vincent, Functional assessment of temperature-gated ion-channel activity using a real-time pcr machine, BioTechniques 47 (3S) (2009) iii–ix, PMID: 19852757.
[10] G.Y. Tang, C. Yang, C.J. Chai, H.Q. Gong, Modeling of electroosmotic flow and capillary electrophoresis with the Joule heating effect: the Nernst-Planck equation versus the Boltzmann distribution, Langmuir 19 (12 2003) 10975–10984.
[11] N.J. Petersen, R.P.H. Nikolajsen, K.B. Mogensen, J.P. Kutter, Effect of Joule heating on efficiency and performance for microchip-based and capillary-based electrophoretic separation systems: a closer look, Electrophoresis 25 (2) (2004) 253–269.
[12] X. Xuan, Joule heating in electrokinetic flow, Electrophoresis 29 (1) (2008) 33–43.
[13] A. Shamloo, A. Merdasi, P. Vatankhah, Numerical simulation of heat transfer in mixed electroosmotic pressure-driven flow in straight microchannels, J. Therm. Sci. Eng. Appl. 8 (2015) 11.
[14] Y. Qiao, B. Tu, B. Lu, Ionic size effects to molecular solvation energy and to ion current across a channel resulted from the nonuniform size-modified pnp equations, J. Chem. Phys. 140 (05 2014) 174102.
[15] W. Im, B. Roux, Ion permeation and selectivity of ompf porin: a theoretical study based on molecular dynamics, Brownian dynamics, and continuum electrodiffusion theory, J. Mol. Biol. 322 (4) (2002) 851–869.
[16] D. Gillespie, W. Nonner, R. Eisenberg, Coupling Poisson-Nernst-Planck and density functional theory to calculate ion flux, J. Phys. Condens. Matter 14 (11 2002) 12129–12145.
[17] G.-W. Wei, Q. Zheng, Z. Chen, K. Xia, Variational multiscale models for charge transport, SIAM Rev. 54 (4) (2012) 699–754.
[18] J.-L. Liu, B. Eisenberg, Poisson-Nernst-Planck-Fermi theory for modeling biological ion channels, J. Chem. Phys. 141 (22) (2014) 22D532.
[19] Z. Xu, M. Ma, P. Liu, Self-energy-modified Poisson-Nernst-Planck equations: Wkb approximation and finite-difference approaches, Phys. Rev. E, Stat. Nonlinear Soft Matter Phys. 90 (1) (2014) 013307.
[20] T.-L. Horng, T.-C. Lin, C. Liu, B. Eisenberg, Pnp equations with steric effects: a model of ion flow through channels, J. Phys. Chem. B 116 (09 2012) 11422–11441.
[21] B. Eisenberg, W. Liu, Poisson-Nernst-Planck systems for ion channels with permanent charges, SIAM J. Math. Anal. 38 (6) (2007) 1932–1966.
[22] A. Flavell, M. Machen, B. Eisenberg, J. Kabre, C. Liu, X. Li, A conservative finite difference scheme for Poisson–Nernst–Planck equations, J. Comput. Electron. 13 (Mar 2014) 235–249.
[23] C. Liu, M. Metti, J. Xu, Energetically Stable Discretizations for Charge Carrier Transport and Electrokinetic Models, 2015.
[24] D. Xie, Y. Jiang, A nonlocal modified Poisson–Boltzmann equation and finite element solver for computing electrostatics of biomolecules, J. Comput. Phys. 322 (2016) 1–20.
[25] E. Feireisl, Mathematical theory of compressible, viscous, and heat conducting fluids, Comput. Math. Appl. 53 (3–4) (2007) 461–490.
[26] M. Bulíček, E. Feireisl, J. Málek, A Navier-Stokes-Fourier system for incompressible fluids with temperature dependent material coefficients, Nonlinear Anal., Real World Appl. 10 (2) (2009) 992–1015.

[27] J. Xu, L. Zikatanov, A monotone finite element scheme for convection-diffusion equations, Math. Comput. 68 (Oct. 1999) 1429–1446.
[28] B. Kirby, Micro- and Nanoscale Fluid Mechanics: Transport in Microfluidic Devices, Cambridge University Press, 2010.
[29] S.C. Brenner, L.R. Scott, The Mathematical Theory of Finite Element Methods, third ed., Texts in Applied Mathematics, vol. 15, Springer, New York, 2008.
[30] P. Ciarlet, The Finite Element Method for Elliptic Problems, Society for Industrial and Applied Mathematics, 2002.
[31] L.C. Evans, Partial Differential Equations, American Mathematical Society, Providence, R.I., 2010.
[32] D. Lide, CRC Handbook of Chemistry and Physics, 85th edition, Taylor & Francis, 2004.
[33] Arthur Bousquet, Xiaozhe Hu, Jinchao Xu, Maximilian S. Metti, Newton solvers for drift-diffusion and electrokinetic equations, SIAM J. Sci. Comput. 40 (2018) B982–B1006.